International Journal of ChemTech Research
CODEN (USA): IJCRGG ISSN: 0974-4290
Vol.7, No.3, pp 1369-1376, 2014-2015

ICONN 2015 [5th -7th Feb 2015]
International Conference on Nanoscience and Nanotechnology-2015
SRM University, Chennai, India

Visible light induced photocatalytic degradation of 2,4-dichlorophenol on ZnO-NiO coupled metal oxides

E.D. Sherly and J. Judith Vijaya*

Catalysis and Nanomaterials Research Laboratory, Dept of Chemistry, Loyola College, Chennai, India.

Abstract: ZnO, NiO and coupled metal oxides in the molar ratio 1:1, 2:1 and 1:2, labeled as ZnNi, Zn_2Ni and $ZnNi_2$, respectively were successfully synthesized by a one-step microwave assisted solution combustion process. As-prepared nano porous metal oxides were characterized by X-ray diffraction (XRD), X-Ray photoelectron spectroscopy (XPS), field emission scanning electron microscopy (FESEM), X-ray energy dispersive spectroscopy (EDS), transmission electron microscopy (TEM), diffuse reflectance spectroscopy (DRS), and photoluminescence spectroscopy (PL). The optical absorption of the samples could be extended into visible region after the loading of NiO. The coupled metal oxide, Zn_2Ni exhibited excellent photocatalytic efficiency towards the removal of 2,4-dichlorophenol from aqueous solution under visible light irradiation, which might be ascribed to the efficient separation of photogenerated electron-hole pairs and to the lowering of band gap on coupling with NiO. Photocatalytic degradation process is found to obey the pseudo-first-order kinetics. This study suggests that the coupled metal oxide, Zn_2Ni could be explored as an efficient material with high efficiency and recyclability for the phtocatalytic degradation of organic pollutants from aqueous solution.
Keywords: photocatalytic degradation, 2,4-dichlorophenol, ZnO-NiO coupled metal oxides.

Introduction

Waste water from industries, such as, petroleum refining and plastics contain large amounts of phenols. The efficient removal of these organic pollutants from water bodies is a challenge facing the global society today. Removal of phenol and chlorinated phenols is important because of their high toxicity and their weak retention in soil sediments[1-3].

Heterogeneous photocatalysis has emerged as an important advanced oxidation process to purify waste water, as it can completely degrade the organic pollutants into water and CO_2, without generating any harmful byproducts. Even though, TiO_2 and ZnO are known for their efficient photocatalytic activity, their wide band gap of around 3.2 eV, which would require an excitation wavelength in the UV region and high electron-hole pair recombination rate limit their photocatalytic efficiency. Coupling of two semiconductors with suitable band gaps can improve the photocatalytic efficiency by delaying the electron–hole pair recombination[4-6].

Among these composite materials, NiO/ZnO coupled systems have been receiving lot of attention, because of the matching electronic band positions of NiO and ZnO[7]. When the coupled photocatalyst, ZnO-

NiO is irradiated by light with the photon energy equal to or higher than the band gaps of ZnO and NiO, the photogenerated electron would transfer from the conduction band of NiO to the conduction band of ZnO and, conversely, the hole would transfer from the valence band of ZnO to the valence band of NiO, leading to a decrease of the electron-hole pairs recombination rate and an increase in their lifetime. Therefore, the formation of NiO-ZnO composites could obviously enhance their photocatalytic activity[8].

Previously, ZnO-NiO coupled metal oxides were prepared by calcining zinc-nickel citrate hollow microspheres[8], impregnation technique[9], by growing NiO nanoparticles on ZnO hierarchical structures[7] and sol-gel method[10]. In the present study, we have prepared the coupled metal oxides of ZnO-NiO through a microwave assisted combustion synthesis. This process involves a self-sustained reaction in the homogeneous solution of different oxidizers (e.g., metal nitrates) and fuels (e.g., urea, glycine, hydrazides). In a microwave assisted combustion synthesis, the microwave induces the rotation of molecular dipoles leading to higher rate of molecular collisions generating enormous amount of heat within the sample. The reaction can be performed in a domestic microwave oven and the operation is clean, fast, less energy consuming and cheap[11-12]. As-prepared coupled metal oxides along with pure ZnO and NiO is used to degrade 2,4-dichlorophenol, a model pollutant in the present study. It has been proved that the coupled metal oxide Zn_2Ni is more efficient towards the degradation of 2,4-dichlorophenol in the aqueous solution under visible light irradiation.

Experimental section

Synthesis of nano ZnO, NiO and coupled ZnO - NiO

All the reagents used were of analytical grade obtained from Merck, India and were used as received without further purification.

For the preparation of ZnO nanoparticles, zinc nitrate ($Zn(NO_3)_2.6H_2O$) and urea (CH_4N_2O) were taken in 1:4 molar ratio and dissolved separately in 10 mL of deionized water, mixed and stirred for one hour to obtain a clear solution. This was placed in a domestic microwave-oven (2.45 GHz and 850 W) for 7 minutes. Initially, the solution boiled and underwent dehydration followed by decomposition with the evolution of gases. When the solution reached the point of spontaneous combustion, it vaporized and instantly became a solid. The obtained solid was washed well with distilled water and ethanol and dried in a hot air oven at 80^0C for 2 h. For the synthesis of nano NiO, same procedure as above was followed, using nickel nitrate. For the synthesis of coupled ZnO and NiO, zinc nitrate and nickel nitrate in 1:1, 2:1 and 1:2 molar ratios respectively were dissolved in deionized water and mixed with required amount of urea and treated in a microwave oven to synthesize coupled ZnO-NiO in 1:1, 2:1 and 1:2 molar ratios and labeled as ZnNi, Zn_2Ni and $ZnNi_2$ respectively.

Characterization of ZnO, NiO and coupled ZnO-NiO

The crystallinity of pure ZnO, NiO and coupled ZnNi, Zn_2Ni and $ZnNi_2$ were determined by using a Philips X'pert X-ray diffractometer with Cu Kα radiation at λ = 1.540 Å.

XPS measurements were obtained on a KRATOS-AXIS 165 instrument equipped with dual aluminum–magnesium anodes using Mg K radiation (hυ=1253.6 eV) operated at 5 kV and 15 mA with pass energy 80 eV and an increment of 0.1 eV. Morphological studies and energy dispersive X-ray analysis of ZnO, NiO and coupled ZnO-NiO have been performed with a Hitachi S-4800 field emission scanning electron microscope. TEM images were recorded with TECNAI FE12 TEM instrument operating at 120 kV. The diffuse reflectance UV–Visible spectra of the samples were recorded using Cary 100 UV–Visible spectrophotometer to estimate their energy band gap. The photoluminescence properties were recorded using Varian Cary Eclipse fluorescence spectrophotometer.

Photocatalytic reactor setup and degradation procedure

PCD experiments were carried out in a Heber Annular type Photoreactor for visible irradiation (300 W Tungsten Halogen lamp is used as the visible light source) as shown in **Figure 1**. A fixed amount of pure ZnO, NiO or coupled ZnO/NiO photocatalyst was added to 100 ml of 2,4-dichlorophenol aqueous solution. The above slurry was stirred for 30 min to reach the adsorption/desorption equilibrium followed by visible light irradiation. Aliquots were withdrawn from the suspension at specific time intervals and centrifuged immediately at 1500 rpm. The extent of phenol degradation was monitored by using a UV-Visible spectrophotometer (Perkin- Elmer, Lamda 25). The PCD efficiency (η) was calculated from the following expression: $\eta = C_0$-

C_t/C_0 *x 100* where, C_0 is the initial concentration of 2,4-dichloro phenol, and C_t, the concentration of 2,4-dichloro phenol after time 't'. To check the stability and reusability of the catalyst, the resulting suspension was centrifuged at the end of the experiment. The separated catalyst was reused for repeated tests. All measurements were repeated twice and the results were reproducible within the experiments errors (±3%).

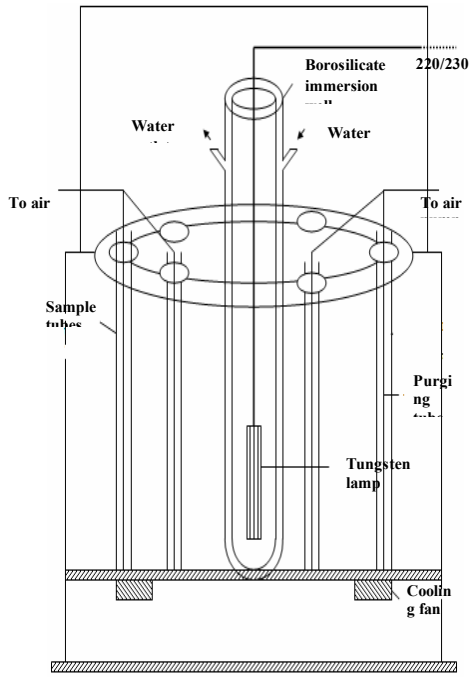

Figure 1. Schematic diagram of the photocatalytic reactor used in the present study

Results and discussion

X-ray diffraction analysis

The XRD patterns of the samples are given in **Figure 2**. For Pure ZnO, the diffraction peaks are located at $2\theta = 31.84^o$, 34.52^o, 36.33^o, 47.63^o, 56.71^o, 62.96^o, 68.13^o, and 69.18^o which are associated with [100], [002], [101], [102], [110], [103], [112] and [201] planes respectively[13]. This pattern has been indexed as hexagonal wurtzite phase of ZnO (JPCDS card number: 36-1451).

The observed diffraction peaks of NiO at $2\theta = 37.26^o$, 43.30^o, 62.89^o, 75.43^o and 79.43^o are associated with [111], [200], [220], [311] and [222] planes respectively [7]. This pattern has been indexed as face centered cubic phase of NiO (JPCDS card number: 78-0643). For the NiO/ZnO coupled systems, two sets of diffraction peaks can be ascribed, to cubic NiO and hexagonal ZnO. It can be deduced from the locations of the peaks that the incorporation of NiO does not lead to a solid solution with ZnO, and the samples ZnNi, Zn_2Ni and $ZnNi_2$ can be regarded as the composite powders of crystalline NiO and ZnO. No characteristic peaks for impurity were observed. Similar XRD pattern was obtained by Tian et al. for the ZnO/NiO heterosystems[7]. The diffraction peaks get broadened on increasing the NiO composition.

The crystallite size of ZnO, NiO and coupled metal oxides was calculated using Debye-Scherrer formula, $\boldsymbol{d = 0.89\lambda / \beta \cos \theta}$[14], where'*d*' is the crystallite size, *0.89*, Scherrer's constant, λ, the wavelength of X-rays, θ, the Bragg diffraction angle, and β, the full width at half-maximum (FWHM) of the diffraction peak. The average crystallite size of pure ZnO was found to be 49 nm, which is derived from the FWHM of most intense peak. The crystallite size of NiO is calculated to be around 8 nm. For the coupled metal oxides, it is 10 - 30 nm. Lowering of the crystallite size on coupling between the two metal oxides is also reported in other preparation methods[15-16].

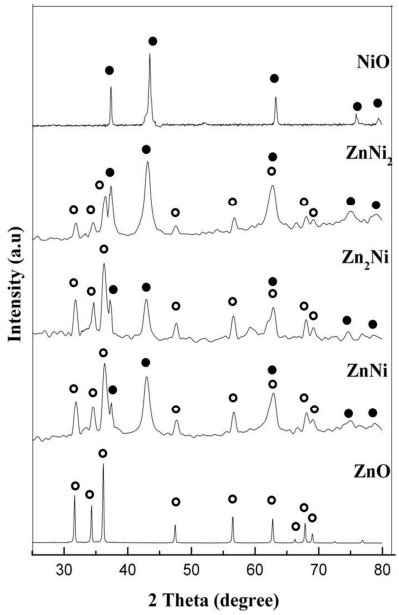

Figure 2. XRD pattern of ZnO, NiO, ZnNi, Zn2Ni and ZnNi2 samples

XPS analysis

XPS is an important surface sensitive analytical technique used for the identification of the surface characteristics of metal oxide nano particles. The typical survey scan of the coupled metal oxide, Zn_2Ni is shown in **Figure 3(a),** which confirms the presence of Zn, Ni, O, and C elements. **Figure 3(b-d)** shows the high-resolution O 1s, Zn 2p and Ni 2p spectra respectively. The high-resolution Zn 2p spectrum (Fig.2.c) displays two major peaks at 1045.6 and 1022.6 eV correspond to the Zn $2p_{3/2}$ and Zn $2p_{1/2}$ energy levels, respectively. The Ni 2p signal as shown in Figure 3 (d) can be de-convoluted into five peaks. The binding energies at 850.2, 856.07, and 863.3 eV were ascribed to the Ni $2p_{3/2}$ peaks, while those at 873.79 and 880.5 eV were attributed to the Ni $2p_{1/2}$ peaks, indicating the presence of Ni^{2+} ions in the coupled metal oxide[8]. From the high resolution scanning XPS spectra of O 1s in Figure 3(b), it can be seen that oxygen on the sample surface exists with binding energies of 531.34 and 532.98 eV, related to the oxygen atom bound to both Ni and Zn atoms[10].

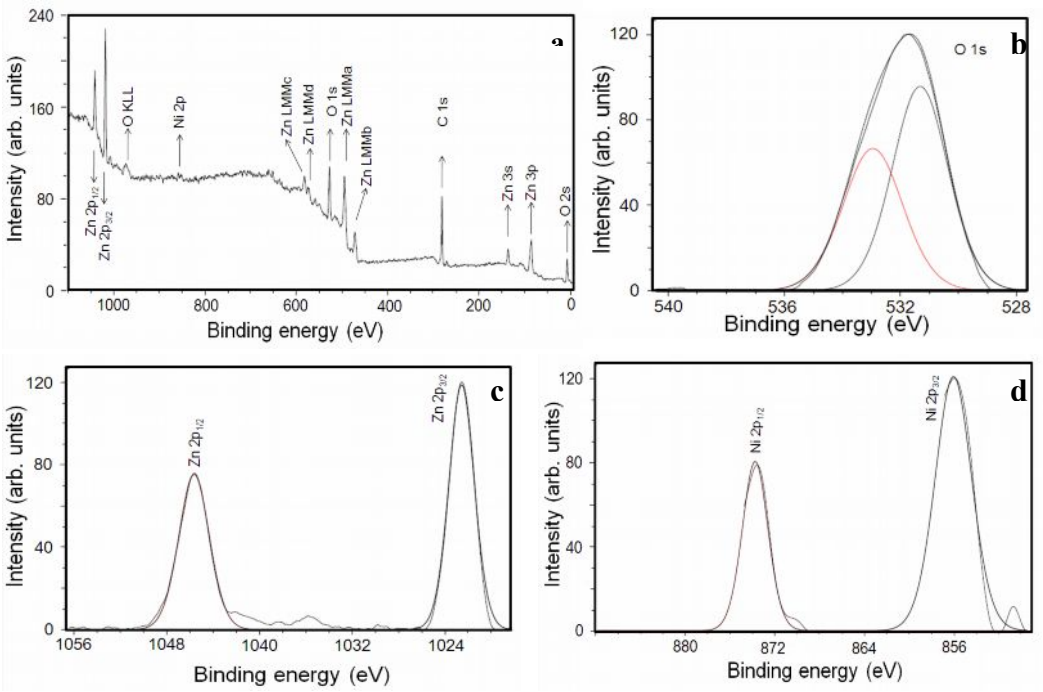

Figure 3. XPS spectra for Zn2Ni (a) survey spectrum and high-resolution (b) O 1s (c) Zn 2p and (d) Ni 2p spectra

Morphology & size analysis

The surface morphology and size of the as-prepared ZnO, NiO and coupled metal oxide, Zn_2Ni was examined by FESEM and TEM analysis. Growth of the nano particles cannot be controlled in the combustion synthesis so that the particles with varying sizes are obtained. **Figure 4 (a**) shows the SEM micrographs of ZnO nanoparticles, which are of irregular spherical shape with varying sizes. **Figures 4 (b)** shows the SEM micrograph of NiO nanoparticles, which are spherical and **Figure 4 (c)** shows the SEM micrograph of coupled metal oxide (Zn_2Ni) nanoparticles. In the coupled metal oxide (Zn_2Ni), NiO nano spheres are embedded on the matrix of ZnO nano particles. The SEM images show that the particles are aggregated, which is due to the enormous heat generated during the combustion reaction. The composition of the prepared ZnO, NiO and coupled metal oxide Zn_2Ni was analyzed by means of energy dispersive x-ray analysis (EDX) as shown in **Figure 5 (a-c).** The EDX result showed the presence of Zn and O, Ni and O and Zn, Ni and O in Figure 5. a, b and c respectively, with the corresponding characteristic peaks and compositions. No other peaks appeared, which shows that the prepared samples are free from impurities.

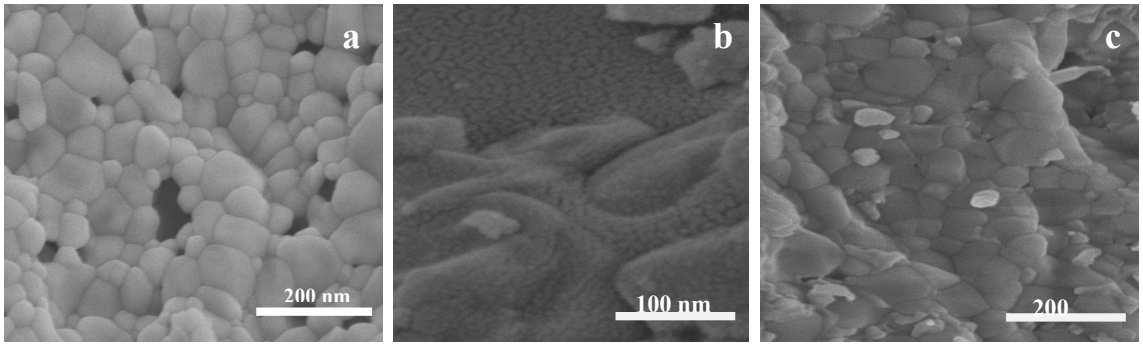

Figure 4. FESEM images of (a) ZnO, (b) NiO (c) Zn2Ni samples

Figure 6 (a, b) shows the TEM images of the ZnO and Zn_2Ni respectively with the SAED pattern given as the inset. ZnO nano particles is roughly spherical and around 40-60 nm in size, which is close to the crystallite size obtained from the XRD analysis. In the coupled metal oxide, Zn_2Ni, the smaller spherical particles of NiO is present in the interstitial spaces of larger darker shaded particles of ZnO. NiO is roughly 10 nm and ZnO is around 30 nm in size and this is in accordance with the crystallite size obtained from XRD analysis. Lowering of particle size is seen in the coupled metal oxide. The polycrystalline nature of ZnO and the coupled metal oxide is revealed from the SAED pattern.

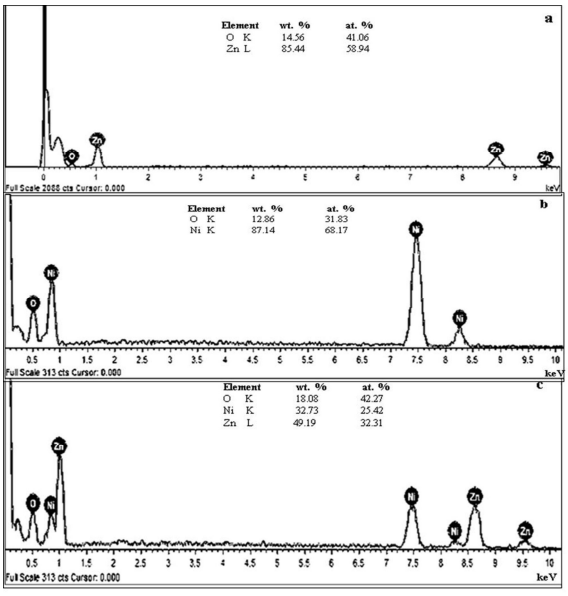

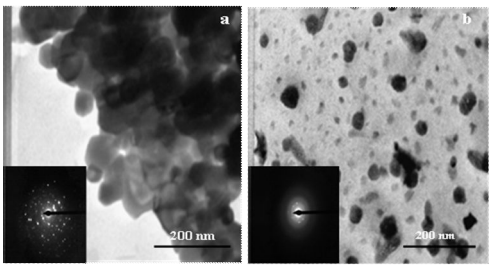

Figure 6. TEM images of (a) ZnO (b) Zn_2Ni samples (SAED pattern is shown as inset)

Figure 5. EDX spectra of a) ZnO, b) NiO c) Zn_2Ni samples

Diffuse reflectance spectroscopy

The band gap energy (Eg) of ZnO, NiO, ZnNi, Zn_2Ni and $ZnNi_2$ was obtained from the optical diffuse reflectance spectra (DRS) recorded at room temperature. The acquired diffuse reflectance spectrum is converted to Kubelka-Munk function. Kubelka-Munk plots are displayed in **Figure 8**. By extrapolating the linear region in the plots of $(f(r)\ h\nu)^2$ versus hν, the value of E_g for ZnO and NiO is found to be 3.12 eV and 3.1 eV respectively, and for ZnNi, Zn_2Ni and $ZnNi_2$, 3.05 eV, 2.85 eV and 3.06 eV respectively. NiO is non-stoichiometric as indicated by the elemental composition obtained from the EDX analysis and its greenish-black color. The addition of NiO alters the absorption edge of ZnO and the absorption wave length of coupled metal oxide, Zn_2Ni is extended towards the visible range with the band gap energy of 2.85 eV. Lower band gap of Zn_2Ni might be caused by the stoichiometry deficiency of ZnO by NiO coupling or due to the formation of defect energy levels[10, 17-18].

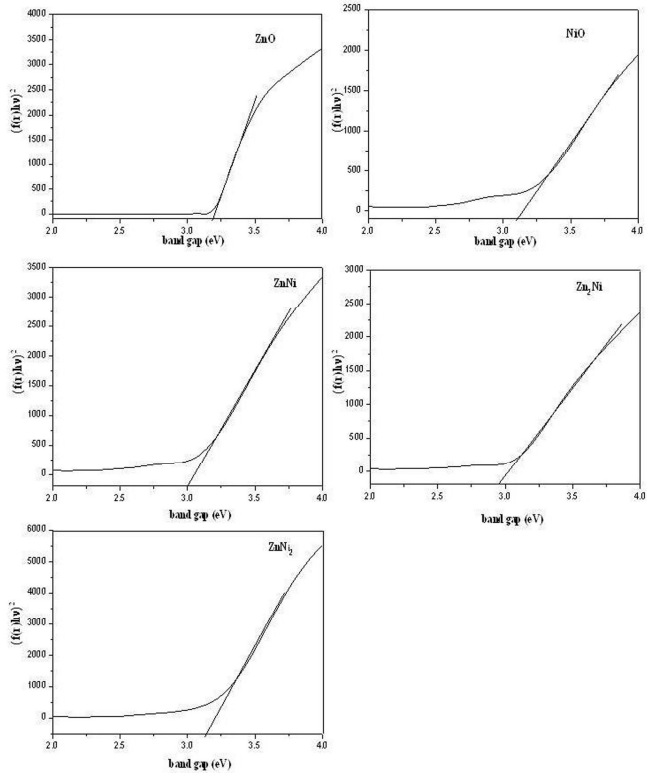

Figure 7. Kubelka-Munk plots of ZnO, NiO, ZnNi, Zn2Ni and ZnNi2 samples

Photoluminescence (PL) emission spectra

PL emission results from the recombination of the photo-induced charge carriers. A weaker PL intensity implies the lower electron–hole recombination rate, and thus higher photocatalytic activity[19]. **Figure 9** displays the PL spectra of ZnO, NiO, ZnNi, Zn_2Ni and $ZnNi_2$ nanoparticles, when the excitation wavelength was 325 nm. The near-band edge UV emission located around 360 and 390 nm results from band–band PL spectrum. The broad visible emissions around 430 nm, 450 nm, and 490-580 nm correspond to the trap-state emission in which the non-radiative transitions of excited elctrons from the CB bottom to the different sub-bands caused by the surface defects like oxygen vacancies occur first, and subsequent radiative transitions from the sub-band to the VB occurs. Oxygen vacancies can promote O_2 adsorbing and the adsorbed O_2 capture photo-induced electrons and thereby simultaneously producing O_2 radical groups. The radical groups are active to promote the oxidation of organic substances[20]. So the oxygen vacancies and the defects are in favor of the photocatalytic reactions.

Figure 9 clearly shows that the pure ZnO has the highest PL intensity, while the coupled metal oxide, Zn_2Ni has the lowest PL intensity. Such PL results indicate that the recombination of the photogenerated electron-hole pairs is suppressed greatly in Zn_2Ni suggesting an efficient separation of photogenerated electron-hole pairs and enhanced photocatalytic activity[21].

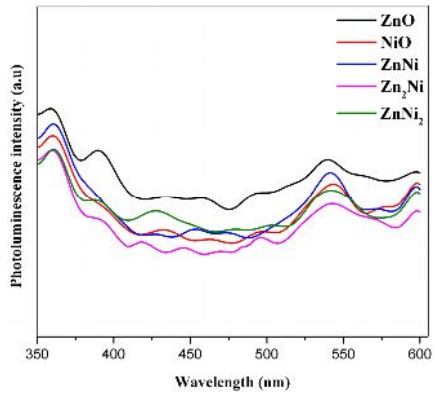

Figure 8. Photoluminescence spectra of ZnO, NiO, ZnNi, Zn2Ni, ZnNi2 samples Photo catalytic activity

Photocatalytic activity of ZnO, NiO and the coupled metal oxides ZnNi, Zn_2Ni and $ZnNi_2$ was evaluated by taking 2,4-DCP as the model pollutant and the degradation studies were carried out under visible light irradiation. The photocatalytic degradation follows the pseudo first order reaction and its kinetics can be expressed using $\ln(C_0/C_t) = kt$, where k is the apparent reaction rate constant, C_0, the initial concentration of 2,4-DCP, t, the reaction time and C_t, the concentration of 2,4-DCP at time t. **Figure 9** shows the kinetic fit for the degradation of 2, 4-DCP over pure ZnO, NiO and coupled ZnNi, Zn_2Ni and $ZnNi_2$ with the catalyst dosage of 50 mg, 2,4-DCP concentration of 50 mg per liter and at pH 7. Maximum degradation (up to 90%) was achieved with the coupled catalyst Zn_2Ni.

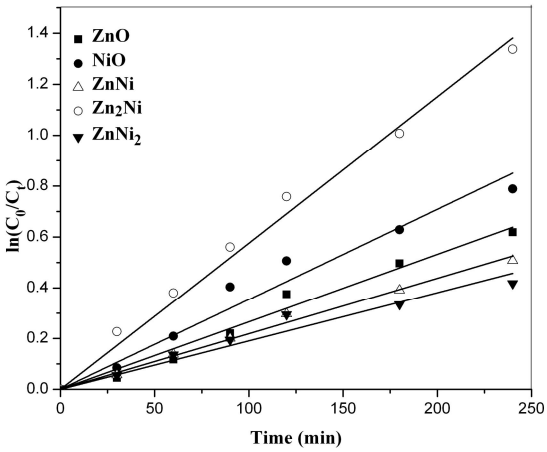

Figure 9. Kinetic fit for ZnO, NiO, ZnNi, Zn2Ni and ZnNi2 structure in NiO-ZnO composite

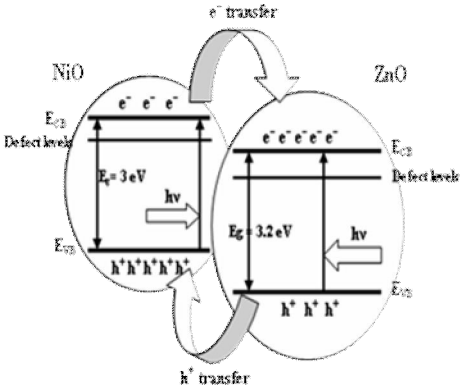

Figure 10. Schematic of the energy band structure in NiO-ZnO composite

Based on the above experimental observations and analysis, we have proposed a mechanism with a schematic energy level diagram to represent the charge transfer process in ZnO-NiO coupled metal oxide for the degradation of 2,4-DCP as given in **Figure 10**. When ZnO-NiO coupled metal oxide is irradiated by visible light, the electrons in the valence band (VB) of ZnO and NiO can be excited to their conduction bands (CB) or to the defect levels present in the band gap. The excited electrons from CB of NiO are transferred to the low lying CB of ZnO. The holes are transferred from the VB of ZnO to the VB band of NiO. This in turn leads to the efficient separation of photogenerated electron-hole pairs. As a result, the photocatalytic activity of the ZnO-NiO coupled metal oxide is significantly enhanced. The efficient visible light photocatalytic degradation shown by the coupled metal oxides could be due to the stoichiometry deficiency induced on coupling and by the formation of defect energy levels[10, 17-18].

Conclusions

Pure ZnO, NiO and their coupled oxides are successfully prepared by a microwave assisted solution combustion synthesis using urea as the fuel. The prepared nano particles are well characterized by XRD, FESEM and EDX, TEM, DRS and PL analysis. This method has formed extremely pure nano particles in good yield. Microwave combustion synthesis has been used for the first time for the preparation of ZnO-NiO coupled

metal oxides. The coupled metal oxide Zn2Ni showed the maximum efficiency towards the degradation of 2,4-dichlorophenol under visible light irradiation. The catalysts exhibited good stability and reusability. The recommended process parameters, such as, the catalyst concentration, phenol concentration and pH are 50 mg per 100 ml of the catalyst, 50 mg per liter of 2,4-DCP and pH around 7.

References:

1. Ollis D F, Turchi C S, Heterogeneous photocatalysis for water purification, Environ. Prog., 1990, 9, 229-234.
2. Hoffmann M R., Martin S T, Choi W, Bahanmann D W, Environmental application of semiconductor photocatalysis, Chem. Rev., 1995, 95, 69-96.
3. Mills A, Hunte S L, An overview of semiconductor photocatalysis, J. Photochem. Photobiol. A chem., 1997, 108, 1-35.
4. Neppolian B, Wang Q, Yamashita H, Choi H, Synthesis and characterization of ZrO_2–TiO_2 binary oxide semiconductor nanoparticles: Application and interparticle electron transfer process, Appl. Catal. A, 2007, 333, 264-271.
5. Robert D, Photosensitization of TiO_2 by M_xO_y and M_xS_y nanoparticles for heterogeneous photocatalysis applications, Catal. Today, 2007, 122, 20-26.
6. Lin X, Huang F, Xing J, Wang W, Xu F, Heterojunction semiconductor SnO_2/$SrNb_2O_6$ with an enhanced photocatalytic activity: The significance of chemically bonded interface, Acta Mater., 2008, 56, 2699-2705.
7. Tian F, Liu Y, Synthesis of p-type NiO/n-type ZnO heterostructure and its enhanced photocatalytic activity, Scripta Mater., 2013, 69, 417–419.
8. Xie Q, Guo H, Zhang X, Lu A, Zeng D, Chen Y, Peng D L, A Facile approach to fabrication of well-dispersed NiO-ZnO composite hollow microspheres, RSC Adv., 2013,3, 24430-24439.
9. Belhadi A, Boumaza S, Trari M, Photoassisted hydrogen production under visible light over NiO/ZnO hetero-system, Appl. Energ., 2011, 88, 4490–4495.
10. Shifu C, Wei Z, Wei L, Sujuan Z, Preparation, characterization and activity evaluation of p–n junction photocatalyst p-NiO/n-ZnO, J. Sol-Gel Sci. Technol., 2009, 50, 387–396.
11. Aruna S T, Mukasyan A S, Combustion synthesis and nanomaterials, Curr. Opin. Solid State Mat. Sci., 2008, 12, 44–50.
12. Bhatte K D, Sawant D N, Watile R A, Bhanage B M, A rapid, one step microwave assisted synthesis of nano size zinc oxide, Mat. Lett., 2012, 69, 66–68.
13. Zhou J, Zhao F, Wang Y, Zhang Y, Yang L, Size-controlled synthesis of ZnO nanoparticles and their photoluminescence properties, J. Lumin., 2007, 122-123,195-197.
14. Cullity B D, Elements of X-ray diffraction, Addison-Wesley, Reading, Mass, USA, 3rd edition, 1967.
15. Liao W, Zheng T, Wang P, Tu S, Pan W, Efficient microwave-assisted photocatalytic degradation of endocrine disruptor dimethyl phthalate over composite catalyst ZrO*x*/ZnO J. Environ. Sci.,2010, 22, 1800–1806.
16. Wang H, Baek S, Lee J, Lim S, High photocatalytic activity of silver-loaded ZnO-SnO_2 coupled catalysts, Chem. Eng. J. 2009, 146, 355–361.
17. Shifu C, Wei Z, Wei L, Sujuan Z, Preparation, characterization and activity evaluation of p–n junction photocatalyst p-ZnO/n-TiO_2, Appl. Surf. Sci., 2008, 255, 2478–2484.
18. Sathishkumar P, Ramaswamy S, Wu J J, Anandan S., Synthesis of CuO-ZnO nanophotocatalyst for visible light assisted degradation of a textile dye in aqueous solution, Chem. Eng. J. 2011, 171, 136–140.
19. Sin J C, Lam S M, Lee K T, Mohamed A. R, Photocatalytic performance of novel samarium-doped spherical-like ZnO hierarchical nanostructures under visible light irradiation for 2,4-dichlorophenol degradation, J. Colloid Interface Sci., 2013, 401 40–49.
20. Liqiang J, Yichun Q, Baiqi W, Shudan L, Baojiang J, Libin Y, Wei F, Honggang F, Jiazhong S, Review of photoluminescence performance of nano-sized semiconductor materials and its relationships with photocatalytic activity, Sol. Energy Mater. Sol. Cells, 2006, 90, 1773–1787.
21. Sakthivel S, Geissen S U, Bahnemanna D W, Murugesan V, Vogelpohl A, Enhancement of photocatalytic activity by semiconductor heterojunctions: Fe_2O_3, WO_3 and CdS deposited on ZnO, J. Photochem. Photobiol. A: Chem., 2002, 148, 283–293.

*****